Liver X receptor activation stimulates iron export in human alternative macrophages.

Gael Bories, Sophie Colin, Jonathan Vanhoutte, Bruno Derudas, Corinne Copin, Melanie Fanchon, Mehdi Daoudi, Loic Belloy, Stephan Haulon, Christophe Zawadzki, et al.

Liver X Receptor (LXR) activation stimulates iron export in human alternative macrophages

G. Bories[1,2,3,4], S. Colin[1,2,3,4], J. Vanhoutte[1,2,3,4], B. Derudas [1,2,3,4], C. Copin[1,2,3,4], M. Fanchon[1,2,3,4], M. Daoudi[1,2,3,4], L. Belloy [1,2,3,4], S. Haulon[5], C. Zawadzki[1,5], B. Jude[1,5], B. Staels[1,2,3,4] and G. Chinetti-Gbaguidi[1,2,3,4]

[1] Université Lille 2, F-59000, Lille, France
[2] Inserm, U1011, F-59000, Lille, France
[3] Institut Pasteur de Lille, F-59019, Lille, France
[4] European Genomic Institute for Diabetes (EGID), FR 3508, F-59000 Lille, France
[5] Centre Hospitalier Régional Universitaire de Lille, France

Bories - LXR controls macrophage iron metabolism

Word count: 5933

Subject codes: [142], [143], [134]

Address correspondence to:
Bart Staels
Inserm UR 1011, Institut Pasteur de Lille
1, rue du Professeur Calmette,
BP 245, Lille 59019, France
Tel: +33-3-20-87-73-88;
Fax: +33-3-20-87-73-60
E-mail : bart.staels@pasteur-lille.fr

ABSTRACT

Rationale – In atherosclerotic plaques, iron preferentially accumulates in macrophages where it can exert pro-oxidant activities.
Objective – The objective of this study is, first, to better characterize the iron distribution and metabolism in macrophage sub-populations in human atherosclerotic plaques and, second, to determine whether iron homeostasis is under the control of nuclear receptors, such as the Liver X Receptors (LXR).
Methods and Results – Here we report that iron depots accumulate in human atherosclerotic plaque areas enriched in CD68 and Mannose Receptor (MR) positive (CD68+MR+) alternative M2 macrophages. *In vitro* IL-4 polarization of human monocytes into M2 macrophages also resulted in a gene expression profile and phenotype favouring iron accumulation. However, upon iron exposure, M2 macrophages acquire a phenotype favouring iron release, through a strong increase in ferroportin expression, illustrated by a more avid oxidation of extra-cellular LDL by iron-loaded M2 macrophages. In line, in human atherosclerotic plaques, CD68+MR+ macrophages accumulate oxidized lipids, which activate Liver X Receptors (LXRα and LXRβ), resulting in the induction of ABCA1, ABCG1 and ApoE expression. Moreover, in iron-loaded M2 macrophages, LXR activation induces nuclear factor erythroid 2-like 2 (NRF2) expression, hence increasing ferroportin expression, which, together with a decrease of hepcidin mRNA levels, promotes iron export.
Conclusions – These data identify a role for M2 macrophages in iron handling, a process which is regulated by LXR activation.

Keywords: Atherosclerosis, macrophages, nuclear receptors, iron

Non standard abbreviations and acronyms

ABC ATP-binding cassette

Apo apolipoprotein

IL interleukin

LCM laser capture microdissection

LDL low-density lipoprotein

LXR liver X receptor

LXRE LXR response element

M1 classically activated macrophages

M2 alternatively polarized macrophages

MR mannose receptor

PFA paraformaldehyde

Q-PCR quantitative polymerase chain reaction

RM resting macrophage

siRNA small interfering RNA

INTRODUCTION

Increasing evidences support a role for cellular iron in the development and progression of atherosclerosis.[1] Epidemiological and experimental studies indicate that atherogenesis is associated with alterations in iron storage and handling in the human body.[2,3] Increased intraplaque iron deposition promotes oxidative stress, protein and lipoprotein oxidation, factors known to affect plaque stability.[4,5]

The main source of redox-active iron in atherosclerotic plaques is the erythrocytes entering the tissue upon intraplaque hemorrhage after microvessel rupture. These erythrocytes are rapidly lysed and phagocytosed leading to the release of hemoglobin, heme and subsequently free iron.[5,6] Most of the iron within vascular lesions is associated with macrophages where it can enhance LDL oxidation, angiogenesis, nitric oxide production, induction of oxidative stress-responsive transcription factors, activation of inflammatory cytokines, and apoptosis.[7,8]

Iron homeostasis in macrophages is determined by the balance of iron uptake through the transferrin receptor (TfR1) and low density lipoprotein receptor-related protein 1 (LRP1), involved in uptake of transferrin or heme associated iron, respectively, and by the solute carrier family 11 (proton-coupled divalent metal ion transporters) member 2 (DMT1), involved in the uptake of non-transferrin bound iron (NTBI),[9,10] and iron release by ferroportin whose expression is controlled by hepcidin and by the transcription factor nuclear factor erythroid 2-like 2 (NRF2) [11]. Iron is stored associated to ferritin heavy chain (FTH) and light chain (FTL), the latter being most efficient,[12] while ceruloplasmin, is a ferroxidase facilitating the transfer of macrophage-released iron to transferrin.

Macrophages are plastic cells which respond to environmental signals (microbial products, damaged cells, activated lymphocytes, cytokines) by acquiring distinct functional phenotypes. While Th1 cytokines (IFNγ and IL1-β) or bacterial LPS induce a "classical" pro-inflammatory profile (M1), Th2 cytokines, such as IL-4 and IL-13, induce an "alternative" anti-inflammatory and reparatory phenotype (M2). Moreover, *in vivo*, several macrophage sub-populations have been identified in human atherosclerotic plaques.[13-14] We have previously identified a population of alternative macrophages co-expressing the pan-macrophage CD68 and the alternative differentiation marker mannose receptor (MR) (CD68+MR+), characterized by a reduced ability to handle lipids, but highly competent for phagocytosis.[13] Moreover, CD68+MR+CD163+ alternative M2 macrophages have been detected in areas of hemorrhage.[15,14] Such macrophages, induced *in vitro* by the haemoglobin/haptoglobin complex, produce anti-inflammatory factors and are protected against lipid accumulation.[15,14]

The objective of this study was, first, to better characterize the iron distribution and metabolism in macrophage sub-populations in human atherosclerotic plaques and, second, to determine whether iron homeostasis is under the control of nuclear receptors, such as the Liver X Receptors (LXR).

MATERIAL AND METHODS

Immunohistochemical analysis

Human atherosclerotic plaques were removed from patients eligible for surgical carotid endarterectomy, recruited at the Cardiovascular Surgery Department (Hospital of Lille, France). Informed consent was obtained from all patients. For immunohistochemical analysis, endogenous peroxidase activity was quenched. Endothelial cells were detected by anti-PECAM1/CD31 (Novus Biological), smooth muscle cells (SMC) by anti-α-actin and macrophages by anti-CD68 antibodies (Dako), using N-Histofine Simple Stain (Nichirei Biosciences Inc.). PECAM1 was revealed by blue staining (BCIP/NBT, Vector), α-actin by grey precipitate (Vector SG) and CD68 by red staining (Vector Nova Red). Adjacent sections were stained with goat polyclonal anti-human MR (SantaCruz) or mouse monoclonal anti-4-Hydroxy-2-Nonenal (4-HNE) (Abcam) antibody. Sections of atherosclerotic plaques positive for CD68+MR+ or CD68+MR- were submitted to laser capture microdissection (LCM) as described.[13] Macrophage-rich areas were captured from 4 adjacent 8 µm-sections and pooled for RNA extraction or for lipid extraction by chloroform/methanol (2:1).

Cell Culture

Human peripheral blood mononuclear cells were isolated from healthy donors by Ficoll density gradient centrifugation. Resting macrophages (RM) were obtained by 6 days of culture in RPMI 1640 medium (Invitrogen, France) supplemented with gentamicin (40 µg/mL), L-glutamine (2 mmol/L) (Sigma-Aldrich, France) and 10% pooled human serum (Abcys, France). To yield alternative differentiated macrophages (M2), recombinant human IL-4 (15 ng/mL, Promocell, Germany) was added at the beginning of differentiation and maintained for 6 days. M1 macrophages were obtained by acute treatment of differentiated RM macrophages with LPS (100 ng/ml, 4h). Where indicated, the LXR agonists T0901317 (T09, 1 µmol/L) and GW3965 (1 µmol/L) were added for 24h in serum free-medium.

Erythrocytes were isolated from autologous blood. The erythrocyte containing phase was washed and centrifuged 3X (2000 rpm, 5 min, 10°C). On the day of use, erythrocytes were incubated for 1h at 37°C with oxidation solution ($CuSO_4$ 0.4 mmol/L and ascorbic acid 5 mmol/L in PBS) to render them senescent and put on macrophages at the ratio of 100 erythrocytes/macrophage.

In vitro erythrophagocytosis assay

RM and M2 macrophages were incubated for 16h with senescent erythrocytes native or labelled with PKH26 fluorescent dye (Sigma) for FACS analysis. Non-ingested erythrocytes were removed by erythrocyte lysis solution (NH_4Cl 140 mmol/L, Tris HCl 17 mmol/L in PBS) and macrophages were incubated for 48h in medium without serum before RNA extraction. For FACS analysis, non-ingested erythrocytes were removed and macrophages directly recovered in PBS-EDTA, filtered with a 80 µm filter, fixed in paraformaldehyde (PFA) 2% in PBS and analysed on a FACS Calibur2 instrument.

RNA extraction and analysis

Total cellular RNA was extracted using Trizol (Life Technologies, France). RNA extraction from LCM-isolated samples was performed using the Picopure RNA extraction kit (MDS Analytical Technologies). RNA quality was assessed using the Agilent 2100 Bioanalyser (Agilent Technologies). Only samples displaying a RNA Integrity Number (RIN) $\geq$ 6, were used further for RNA analysis. RNA was amplified in two rounds using the ExpressArt TRinucleotide mRNA amplification Nano kit (AmpTec GmbH). For quantitative PCR (Q-PCR), RNA was reverse transcribed using random hexamer primers and Superscript reverse transcriptase (Life Technologies, France) and cDNAs were quantified on a MX3000 apparatus (Stratagene) using specific primers (supplemental table 1). mRNA levels were normalized to those of cyclophilin.

Small interfering RNA–mediated RNA interference

Small interfering (si)RNA oligonucleotides corresponding to human LXRα, LXRβ, NRF2, ferroportin (Dharmacon) and scrambled control RNA (Ambion) were used. M2 macrophages were transfected

using Dharmafect4 reagent (Dharmacon) and then treated for a further 24h in the absence or in the bpresence of T09 (1 µmol/L) or $FeCl_3$ (100 µmol/L).

Measurement of iron content by the ferrozine assay
RM and M2 macrophages were loaded or not with iron ($FeCl_3$ 100 µmol/L, Sigma-Aldrich) in serum-containing medium for 24h. Cellular extracts were obtained in NaOH 50 mmol/L and stored for iron quantification. In the iron release experiment, iron-loaded RM and M2 macrophages were incubated in serum free- medium containing or not T09 (1 µmol/L) for different time periods as indicated. In ferroportin siRNA experiments, cells were transfected before iron loading. Iron quantification in cellular extracts and medium was performed using the ferrozine assay.[16] Cell culture medium was dried (65°C, 24h) and rehydrated by addition of 100 µL of NaOH 50 mmol/L before iron quantification. Iron release was calculated as (iron medium)/(iron medium + iron in cells) x 100.

Ferritin immunostaining
RM and M2 macrophages were treated with $FeCl_3$ (100 µmol/L) for 24h, washed with PBS, fixed with PFA (4% in PBS) for 15 min and then incubated overnight with an anti-human ferritin antibody (Acris). After washing, cells were incubated for 30 min at room temperature with N-Histofine Simple Stain conjugated with anti-rabbit immunoglobulin G.

Perls staining
Iron deposition was revealed by Perls Prussian blue staining in the presence or in the absence of 0.5% 3,3α-diaminobenzidine (DAB) for 20 min.

Flow cytometry analysis of ferroportin
Unloaded or iron-loaded RM and M2 macrophages were incubated with a rabbit polyclonal anti-ferroportin antibody (ab85370, Abcam) and a phycoerythrin (PE)-labeled goat anti-rabbit secondary antibody (A21428, Molecular probes). Cells were analyzed using FACScalibur™ (BD Biosciences) and data processed with FlowJo xV software.

Lipoprotein preparation and measure of LDL oxidation
LDL ($1.030<d<1.063$ g/mL) was isolated by sequential ultracentrifugation from plasma of fasted normolipidemic donors.[17] Iron-loaded RM and M2 macrophages were incubated in RPMI medium containing native LDL (1 mg/ml) for 24h. LDL was then isolated from the supernatant by ultracentrifugation and conjugated dienes measured by spectrophotometry at 234 nm as described.[18] The LDL electrophoretic mobility was determined by migration on Cellogel (Sebia) and visualized by Ponceau Red staining. Cupper-oxidized LDL (OxLDL) and native (nLDL, without cell contact) were used as positive and negative controls, respectively.

Protein extraction and western blot analysis
Proteins were extracted with hypotonic buffer (50 mmol/L Hepes, pH 7.8, 10 mmol/L KCl, $MgCl_2$ 2 mmol/L, EDTA 0.1mmol/L, 3 mmol/L DTT, 50 mmol/L NaF, 10 mmol/L $Na_4P_2O_7$, 1 mmol/L Na_3VO_4 and protease inhibitors) added with 0.75 % of NP40. After centrifugation (5 min, 11000 rpm) the supernant was recovered as cytoplasmic fraction whereas hypertonic buffer (50 mmol/L Hepes, pH 7.8, 50 mmol/L KCl, 300 mmol/L NaCl, 10% glycerol, 3 mmol/L DTT, and protease inhibitors) was added to the pellet. After centrifugation (10 min, 14000 rpm), the supernatant was collected as nuclear fraction. Proteins were separated by SDS-PAGE, transferred to Hybond-C Extra membranes (Amersham) and immunoblotted using antibodies against human NRF2, β-actin or lamin A/C (Santa Cruz Biotechnology). After incubation with a secondary peroxidase-conjugated antibody (Santa Cruz Biotechnology), immunoreactive bands were revealed using a chemiluminescence ECL detection kit (Amersham) and quantified by densitometry using the Quantity One software.

Transient transfections

COS cells were transfected with the reporter $(LXRE)_3$-TK-pGL3 and expression (pCMX-empty or pCMX-hLXRα) vectors using jetPEI (Polyplus transfection, France). Subsequently, cells were incubated for an additional 24h with non-fluorescent or autofluorescent oxidized lipids extracted from human atherosclerotic lesions. Luciferase and β-galactosidase activities were measured.

Statistical analysis

Statistical differences between groups were analyzed by ANOVA and Student t-test and considered significant when $P<0.05$.

RESULTS

Iron depots colocalize with M2 macrophages in human atherosclerotic plaques

Within cells of the atherosclerotic plaques, iron preferentially accumulates in macrophages.[19] Given that different macrophage sub-populations are present in human atherosclerotic plaques, we determined whether iron distribution differs between CD68+MR+ M2 macrophages and the CD68+MR- macrophages which resemble *in vitro* resting macrophages (RM).[13] Perls staining followed by intensity signal quantification revealed that iron deposits (stained in blue) co-localize almost exclusively with the CD68+MR+ macrophages in human atherosclerotic plaques (figure 1A,B). These iron-loaded CD68+MR+ macrophages are abundant in areas of neo-vascularization, as indicated by the positive PECAM-1/CD31 endothelial cell staining (figure 1A), likely resulting from the delivery of erythrocytes through intraplaque hemorrhages after microvessel rupture [20].

M2 macrophages are more efficient in iron loading than RM macrophages

Since CD68+MR+, but not CD68+MR- macrophages colocalize with iron depots *in vivo*, the ability of M2 macrophages to accumulate iron was assessed using an *in vitro* model. The expression of genes mediating iron uptake, TfR1, LRP1, DMT1 was more abundant in M2 macrophages compared to RM macrophages (figure 2A-C and online figure IA-C). FTH expression was higher in RM macrophages, whereas FTL, more efficient in iron storage, was higher in M2 macrophages (figure 2D and online figure ID,E). Moreover, ferroportin and ceruloplasmin, genes involved in iron release, were less expressed in M2 macrophages (figure 2F and online figure IF-G), whereas expression of hepcidin, which degrades ferroportin, was very high in M2 macrophages (figure 2E and online figure IH).

To assess whether these differences in gene expression are functional, RM and M2 macrophages were loaded with increasing concentrations of $FeCl_3$. M2 macrophages presented an increased iron deposition, visualized by Pearls staining as brown granules and quantified by the ferrozine assay (online figure II,L). In line, ferritin granules were more abundant in M2 compared to RM macrophages (online figure IM). These results indicate that M2 macrophages display a higher ability to accumulate and store iron compared to RM macrophages.

Iron-loading of M2 macrophages induces a response promoting iron release

Since M2 macrophages display a high iron accumulation capacity, the response of these cells to iron on the expression of genes involved in iron metabolism was analyzed next. Interestingly, iron exposure induced a more pronounced response of M2 compared to RM macrophages as demonstrated by the decrease of TfR1, LRP1, DMT1 and increase of FTL mRNA in M2 compared to RM macrophages (figure 2A-D). Hepcidin more pronouncedly decreased upon iron-loading in M2 compared to RM macrophages, whereas ferroportin expression increased (figure 2E,F). Interestingly, time course experiments indicate that the induction of ferroportin expression by iron in M2 macrophages occurs later than the reduction of hepcidin expression (online figure II). Expression of HMOX-1 and NRF2, markers of oxidative stress, increased also more pronouncedly in M2 macrophages (figure 2G,H).

Similar gene expression regulations were observed upon incubation with senescent erythrocytes (online figure III), indicating that M2 macrophages are more efficient in iron handling than RM macrophages, independently of the iron source. Experiments performed on iron-loaded LPS-activated M1 macrophages indicate that their gene expression profile is intermediary between RM and M2 macrophages (online figure IV). Finally, iron-containing CD68+MR+ macrophage-enriched areas of human atherosclerotic plaques isolated by LCM displayed higher expression of NRF2, hepcidin, and ferroportin than CD68+MR- macrophage enriched zones (online figure V) thus corroborating the *in vitro* results on iron-loaded M2 macrophages.

Induction of ferroportin protein upon iron loading was stronger in M2 compared to RM macrophages, as illustrated by FACS analysis (figure 3A). In line, iron-loaded M2 macrophages released more iron compared to RM macrophages (figure 3B). Moreover, while the % of iron release is similar between RM and M2 macrophages at short time periods, given the fact that M2 macrophages accumulate more iron than RM macrophages, the absolute amount of iron released is significantly higher in M2 than RM macrophages (online figure VI). Altogether, these results suggest that M2 macrophages are more

sensitive to iron loading and adapt their response to deal with the iron-induced oxidative damages by inducing mechanisms to release iron when an excess of iron accumulates.
To determine whether the enhanced iron release by M2 macrophages has functional consequences, the ability of RM and M2 macrophages to oxidize native LDL (nLDL) was determined. LDL incubated with iron-loaded M2 macrophages displayed higher concentrations of conjugated dienes as well as a higher electrophoretic mobility than LDL exposed to iron-loaded RM macrophages (Figure 3C,D), indicating a stronger degree of oxidation.

Iron loading promotes the formation of oxidized lipids which induce LXRα transcriptional activity

Interestingly, iron deposits co-localize with oxidized lipids in atherosclerotic plaques.[21] Therefore, we determined whether CD68+MR+ macrophages accumulate oxidized lipids *in vivo*. Lipid autofluorescence and 4-HNE staining, both markers of oxidation,[22] colocalized with iron-positive CD68+MR+ macrophages, being almost absent in CD68+MR- macrophages (Figure 4A).
Since iron loading can generate oxysterols,[23] natural ligands for LXR,[24,25] the ability of autofluorescent oxidized lipids in atherosclerotic plaques to modulate LXR transcriptional activity was tested. Therefore, LXRE reporter and human LXRα expression plasmid transfected COS cells were treated with autofluorescent oxidized, or control non-fluorescent lipids extracted from atherosclerotic plaques. Autofluorescent oxidized lipids from CD68+MR+ macrophage-rich areas, but not neutral lipids from CD68+MR- macrophage-rich areas of atherosclerotic plaques increased LXRα transcriptional activity (Figure 4B). In line, iron loading of M2 macrophages *in vitro* resulted in increased expression of the LXR target genes ABCA1, ABCG1 and ApoE (Figure 4D-F). siRNA knockdown experiments demonstrated that this regulation was dependent on LXRα (Figure 4C-F), but not on LXRβ (online figure VII). Altogether these results show that iron loading activates LXRα transcriptional activity probably by promoting oxysterol formation.

LXRα activation increases iron export in iron-loaded M2 macrophages

Since iron loading activates LXRα, the effect of LXR activation on macrophage iron metabolism was determined. Among genes involved in iron uptake, storage and export, the expression of ferroportin and hepcidin was significantly regulated by the LXR agonists T0901317 and GW3965 (online figure VIII). siRNA knockdown experiments demonstrated that these effects are mediated by LXRα and not by LXRβ (figure 5A-F). Moreover, siRNA experiments show that LXRα, but not LXRβ, mediates the induction of hepcidin and ferroportin expression by iron loading (figure 5G,H and online figure IX).
Next, we tested whether LXR activation stimulates iron release. M2 macrophages were loaded for 24h with $FeCl_3$ and treated for a further 24h with T0901317. LXR activation enhanced iron release from iron-loaded M2 macrophages (figure 6A). Interestingly, ferroportin-silencing before iron loading, leading to an approximately 65% reduction of ferroportin mRNA (figure 6B), affected basal and blocked the induction of iron release by LXR activation, indicating that the effects of LXR are mediated by ferroportin induction (figure 6A).
Since no putative LXRE sites were found by *in silico* bio-informatic analysis in the human ferroportin promoter, we tested whether the NRF2 pathway is regulated by LXR. Treatment with T0901317 increased NRF2 mRNA and protein levels in the nuclear fraction of M2 macrophages (online figure VIII and figure 7A,B). siRNA knockdown experiments demonstrated that the induction of ferroportin mRNA by T0901317 was abolished by NRF2 silencing (figure 7C).

Erythrophagocytosis induces LXR target gene expression in M2 macrophages.

Given that erythrocytes are the major source of iron in atherosclerotic plaques,[20] the capacity of RM and M2 macrophages to uptake senescent erythrocytes was studied. In line with their stronger ability to accumulate iron, erythrophagocytosis was higher in M2 than RM macrophages (figure 8A). Moreover, erythrocyte uptake increased ABCA1, ABCG1, ApoE and ferroportin expression (figure 8B-E).

DISCUSSION

Neo-vascularization is commonly found in atherosclerotic plaques and can lead to intraplaque hemorrhage after vessel rupture. Rupture of microvessels releases erythrocytes which can be phagocytosed by macrophages, thus leading to an increase in iron content associated with oxidized lipid deposition.[21,26] Moreover, erythrocytes can rapidly lyse thus releasing hemoglobin, which upon oxidization releases heme. This latter can be oxidatively cleaved thus releasing highly reactive free iron.[6,5] Unbound iron can oxidize lipids and induce cell death thus potentially promoting atherosclerosis progression. By contrast, iron bound to ferritin or transferrin is less reactive.[27,28]

Previously, we reported the presence of a CD68+MR+ macrophage subpopulation in human atherosclerotic plaques which closely resembles *in vitro* IL-4-polarized M2 macrophages , which are distinct from the CD68+MR- subpopulation by morphology, localization and function.[29,13] Immunohistological analysis showed that CD68+MR+ macrophages co-localize with iron deposits, whereas CD68+MR- macrophages are poor in iron, suggesting functional differences in terms of iron handling. *In vitro* studies on IL-4 polarized M2 macrophages showed that M2 macrophages display an expression profile favoring iron uptake and storage and disfavoring iron release, suggesting that M2 macrophages have a high capacity to accumulate iron. Accordingly, ferritin expression and iron content was higher in M2 macrophages compared to RM macrophages after iron loading in line with the histological observations in plaques.

Interestingly, after iron exposure, M2 macrophages completely changed their phenotype and acquired a phenotype oriented to iron release, whereas RM were less responsive. In particular, ferroportin expression was strongly increased in M2 macrophages in response to iron. In line, iron-loaded M2 macrophages released more iron than iron-loaded RM macrophages. This observation is in agreement with previous results obtained in human and mouse alternative macrophages differentiated in the presence of M-CSF and IL-4 for 2 days.[30,31] Interestingly, we found that M2 macrophages also phagocytose erythrocytes more avidly than RM macrophages.

The iron handling ability of M2 macrophages suggests a modulatory role of these macrophages in atherosclerosis. Indeed by their increased ability to take up iron from the medium or to phagocyte senescent erythrocytes, associated to their dynamic regulatory response enhancing the release of iron, M2 macrophages could play a role in the recycling of potential detrimental iron and to present it under a less active form, such as bound to ferritin or to transferrin. Iron exported by ferroportin is normally bound to transferrin and thus exempt of oxidative capacity. Although human macrophages do not synthesize transferrin,[32] we speculate that transferrin in atherosclerotic lesions could accept and bind macrophage-excreted iron.[33]

Interestingly, autofluorescent oxidized lipids isolated from CD68+MR+ enriched-areas of human atherosclerotic plaques are able to activate LXRα, in line with data reporting that *in vitro* iron loading generates oxysterols, which are natural ligands for LXR.[23,34] In agreement, iron treatment induces LXR target genes in a LXRα-dependent manner. These genes are also induced upon erythrophagocytosis suggesting that iron, independently of the way of its acquisition, is able to induce LXRα target genes.

Furthermore, we identify a novel role for LXRα in the regulation of macrophage iron homeostasis. Indeed, treatment of alternative macrophages with T0901317 leads to an increased iron release due to the opposite regulation of ferroportin and NRF2, on the one hand, and hepcidin expression, on the other hand, which occurs in a LXRα-dependent manner. Interestingly, we also found that the regulation of several genes involved in iron metabolism after iron exposure is under the control of LXRα. Indeed, LXRα siRNA decreased the expression of ferroportin and NRF2 induced by iron loading, indicating that some physiological effects of iron can occur through the activation of LXRα pathways (online figure X). In the regulation of iron metabolism, similar as reported for cholesterol efflux,[35,13] we did not observe any compensatory effect of LXRβ activation, suggesting that LXRβ probably plays a minor role in the control of these human macrophage functions. We have previously shown that M2 macrophages express lower levels of LXRα compared to RM macrophages, accompanied by lower cholesterol efflux capacities [13]. Here, we report that activation of LXRα pathway regulates iron metabolism promoting iron export in M2 macrophages. These data clearly show that, despite a lower expression of LXRα in M2 compared to RM macrophages, this nuclear receptor specifically regulates pathways, ie iron export in M2 macrophages, emphasising the

functional differences between both macrophage sub-types, and identifying a novel functional role for LXRα specifically in M2 macrophages.

The fact that iron induces the production of LXR agonists, which in turn enhance the release of excess iron, could constitute a protective mechanism in which LXRα plays a role as central regulator. Moreover, LXRα-dependent increased expression of genes involved in cholesterol efflux after iron loading could thus represent a mechanism by which macrophage lipid content is decreased to protect them from detrimental oxidation due to iron accumulation.

Recently, a sub-population of CD68+MR+CD163+ alternative M2 macrophages has been detected in areas of hemorrhage in human atherosclerotic plaques.[15] Such M(Hb) macrophages, obtained *in vitro* upon incubation with the hemoglobin/haptoglobin complex, display reduced intracellular iron content through up-regulation of ferroportin which in turn increases expression of ABC transporters and cholesterol efflux, at least partially via LXRα.[15] By contrast, we show that increased iron content in IL-4 polarized M2 macrophages enhances the expression of ABCA1/ABCG1 through an LXRα-dependent mechanism. In line, heme-directed monocyte differentiation, giving rise to the so-called Mhem macrophages, is characterized by the induction of the activating transcription factor-1 (ATF-1) as well as HMOX-1 and LXRβ, this latter inducing the expression of both LXRα and ABCA1. These macrophages, which are formed in adaptation to intraplaque hemorrhage, are protected from oxidative stress and are less prone to accumulate lipids and to transform into foam cells.[36] However, we found that iron loading increases ABCA1 expression, as well as iron export mechanisms, through a direct activation of LXRα, independent of LXRβ.

While the molecular mechanisms appear different, the final lipid phenotype of these macrophage subtypes seems very similar. Thus we cannot exclude that in human atherosclerotic plaques these macrophages can exist together in areas of neo-vascularization/hemorrhage. It is also tempting to speculate that the presence of these different macrophage subtypes can change during atherosclerotic plaque progression, with macrophages of the phenotype reported here as a first line of defence against senescent erythrocytes and iron caused damages.

In conclusion, we show that M2 macrophages are highly specialized in iron handling and that iron loading drives the activation of LXRα and the transcription of its target genes involved in cholesterol efflux. For the first time, we demonstrate that macrophage iron metabolism is regulated by LXRα activation. Activation of LXRα could modulate atherosclerosis, not only by promoting lipid efflux or decreasing inflammation of macrophages, but also by enhancing their iron recycling capacities through increasing iron release.

ACKNOWLEDGMENTS
We thank Genfit SA (Loos, France) for providing the T0901317 and GW3965 compounds.

SOURCES OF FUNDINGS
Grants from the Région Nord-Pas de Calais/FEDER (CPER N. 1449), the Agence Nationale de la Recherche, France (AlMHA project), the Fondation de France, the Fondation pour la Recherche Médicale, the transatlantic Leducq HDL Network, the "European Genomic Institute for Diabetes" (EGID, ANR-10-LABX-46) are acknowledged. G. Chinetti-Gbaguidi is a recipient of a Contrat d'Interface from the CHRU de Lille. B. Staels is a member of the Institut Universitaire de France.

DISCLOSURES
None

REFERENCES

1. Stadler N, Lindner RA, Davies MJ. Direct detection and quantification of transition metal ions in human atherosclerotic plaques: evidence for the presence of elevated levels of iron and copper. *Arterioscler Thromb Vasc Biol*. 2004;24:949–954.

2. Ramakrishna G, Rooke TW, Cooper LT. Iron and peripheral arterial disease: revisiting the iron hypothesis in a different light. *Vasc Med*. 2003;8:203–210.

3. Yuan X-M, Li W. The iron hypothesis of atherosclerosis and its clinical impact. *Ann Med*. 2003;35:578–591.

4. Lioupis C, Barbatis C, Drougou A, Koliaraki V, Mamalaki A, Klonaris C, Georgopoulos S, Andrikopoulos V, Bastounis E. Association of haptoglobin genotype and common cardiovascular risk factors with the amount of iron in atherosclerotic carotid plaques. *Atherosclerosis*. 2011;216:131–138.

5. Lapenna D, Pierdomenico SD, Ciofani G, Ucchino S, Neri M, Giamberardino MA, Cuccurullo F. Association of body iron stores with low molecular weight iron and oxidant damage of human atherosclerotic plaques. *Free Radic Biol Med*. 2007;42:492–498.

6. Nagy E, Eaton JW, Jeney V, Soares MP, Varga Z, Galajda Z, Szentmiklósi J, Méhes G, Csonka T, Smith A, Vercellotti GM, Balla G, Balla J. Red cells, hemoglobin, heme, iron, and atherogenesis. *Arterioscler Thromb Vasc Biol*. 2010;30:1347–1353.

7. Cromheeke KM, Kockx MM, De Meyer GR, Bosmans JM, Bult H, Beelaerts WJ, Vrints CJ, Herman AG. Inducible nitric oxide synthase colocalizes with signs of lipid oxidation/peroxidation in human atherosclerotic plaques. *Cardiovasc Res*. 1999;43:744–754.

8. Sindrilaru A, Peters T, Wieschalka S, Baican C, Baican A, Peter H, Hainzl A, Schatz S, Qi Y, Schlecht A, Weiss JM, Wlaschek M, Sunderkötter C, Scharffetter-Kochanek K. An unrestrained proinflammatory M1 macrophage population induced by iron impairs wound healing in humans and mice. *J Clin Invest*. 2011;121:985–997.

9. Lane DJR, Robinson SR, Czerwinska H, Bishop GM, Lawen A. Two routes of iron accumulation in astrocytes: ascorbate-dependent ferrous iron uptake via the divalent metal transporter (DMT1) plus an independent route for ferric iron. *Biochem J*. 2010;432:123–132.

10. Gunshin H, Mackenzie B, Berger UV, Gunshin Y, Romero MF, Boron WF, Nussberger S, Gollan JL, Hediger MA. Cloning and characterization of a mammalian proton-coupled metal-ion transporter. *Nature*. 1997;388:482–488.

11. Nemeth E, Tuttle MS, Powelson J, Vaughn MB, Donovan A, Ward DM, Ganz T, Kaplan J. Hepcidin regulates cellular iron efflux by binding to ferroportin and inducing its internalization. *Science*. 2004;306:2090–2093.

12. Levi S, Yewdall SJ, Harrison PM, Santambrogio P, Cozzi A, Rovida E, Albertini A, Arosio P. Evidence of H- and L-chains have co-operative roles in the iron-uptake mechanism of human ferritin. *Biochem J*. 1992;288:591–596.

13. Chinetti-Gbaguidi G, Baron M, Bouhlel MA, Vanhoutte J, Copin C, Sebti Y, Derudas B, Mayi T, Bories G, Tailleux A, Haulon S, Zawadzki C, Jude B, Staels B. Human atherosclerotic plaque alternative macrophages display low cholesterol handling but high phagocytosis because of distinct activities of the PPARγ and LXRα pathways. *Circ Res*. 2011;108:985–995.

14. Boyle JJ, Harrington HA, Piper E, Elderfield K, Stark J, Landis RC, Haskard DO. Coronary intraplaque hemorrhage evokes a novel atheroprotective macrophage phenotype. *Am J Pathol*. 2009;174:1097–1108.

15. Finn AV, Nakano M, Polavarapu R, Karmali V, Saeed O, Zhao X, Yazdani S, Otsuka F, Davis T, Habib A, Narula J, Kolodgie FD, Virmani R. Hemoglobin directs macrophage differentiation and prevents foam cell formation in human atherosclerotic plaques. *J Am Coll Cardiol*. 2012;59:166–177.

16. Riemer J, Hoepken HH, Czerwinska H, Robinson SR, Dringen R. Colorimetric ferrozine-based assay for the quantitation of iron in cultured cells. *Anal Biochem*. 2004;331:370–375.

17. Havel RJ, Eder HA, Bragdon JH. The distribution and chemical composition of ultracentrifugally separated lipoproteins in human serum. *J Clin Invest*. 1955;34:1345–1353.

18. Jenkins AJ, Klein RL, Chassereau CN, Hermayer KL, Lopes-Virella MF. LDL from patients with well-controlled IDDM is not more susceptible to in vitro oxidation. *Diabetes*. 1996;45:762–767.

19. Yuan XM. Apoptotic macrophage-derived foam cells of human atheromas are rich in iron and ferritin, suggesting iron-catalysed reactions to be involved in apoptosis. *Free Radic Res*. 1999;30:221–231.

20. Kolodgie FD, Gold HK, Burke AP, Fowler DR, Kruth HS, Weber DK, Farb A, Guerrero LJ, Hayase M, Kutys R, Narula J, Finn AV, Virmani R. Intraplaque hemorrhage and progression of coronary atheroma. *N Engl J Med*. 2003;349:2316–2325.

21. Lee FY, Lee TS, Pan CC, Huang AL, Chau LY. Colocalization of iron and ceroid in human atherosclerotic lesions. *Atherosclerosis*. 1998;138:281–288.

22. Esterbauer H, Jürgens G, Quehenberger O, Koller E. Autoxidation of human low density lipoprotein: loss of polyunsaturated fatty acids and vitamin E and generation of aldehydes. *J Lipid Res*. 1987;28:495–509.

23. Hascalovici JR, Song W, Vaya J, Khatib S, Fuhrman B, Aviram M, Schipper HM. Impact of heme oxygenase-1 on cholesterol synthesis, cholesterol efflux and oxysterol formation in cultured astroglia. *J Neurochem*. 2009;108:72–81.

24. Janowski BA, Willy PJ, Devi TR, Falck JR, Mangelsdorf DJ. An oxysterol signalling pathway mediated by the nuclear receptor LXR alpha. *Nature*. 1996;383:728–731.

25. Zhao C, Dahlman-Wright K. Liver X receptor in cholesterol metabolism. *J Endocrinol*. 2010;204:233–240.

26. Kockx MM, Cromheeke KM, Knaapen MWM, Bosmans JM, De Meyer GR, Herman AG, Bult H. Phagocytosis and macrophage activation associated with hemorrhagic microvessels in human atherosclerosis. *Arterioscler Thromb Vasc Biol*. 2003;23:440–446.

27. Hollander W, Colombo MA, Kirkpatrick B, Paddock J. Soluble proteins in the human atherosclerotic plaque. With spectral reference to immunoglobulins, C3-complement component, alpha 1-antitrypsin and alpha 2-macroglobulin. *Atherosclerosis*. 1979;34:391–405.

28. Li W, Xu L-H, Forssell C, Sullivan JL, Yuan X-M. Overexpression of transferrin receptor and ferritin related to clinical symptoms and destabilization of human carotid plaques. *Exp Biol Med (Maywood)*. 2008;233:818–826.

29. Bouhlel MA, Derudas B, Rigamonti E, Dièvart R, Brozek J, Haulon S, Zawadzki C, Jude B, Torpier G, Marx N, Staels B, Chinetti-Gbaguidi G. PPARgamma activation primes human monocytes into alternative M2 macrophages with anti-inflammatory properties. *Cell Metab*. 2007;6:137–143.

30. Recalcati S, Locati M, Marini A, Santambrogio P, Zaninotto F, De Pizzol M, Zammataro L, Girelli D, Cairo G. Differential regulation of iron homeostasis during human macrophage polarized activation. *Eur J Immunol*. 2010;40:824–835.

31. Corna G, Campana L, Pignatti E, Castiglioni A, Tagliafico E, Bosurgi L, Campanella A, Brunelli S, Manfredi AA, Apostoli P, Silvestri L, Camaschella C, Rovere-Querini P. Polarization dictates iron handling by inflammatory and alternatively activated macrophages. *Haematologica*. 2010;95:1814–1822.

32. Moura E, Noordermeer MA, Verhoeven N, Verheul AF, Marx JJ. Iron release from human monocytes after erythrophagocytosis in vitro: an investigation in normal subjects and hereditary hemochromatosis patients. *Blood*. 1998;92:2511–2519.

33. Stastny J, Fosslien E, Robertson AL Jr. Human aortic intima protein composition during initial stages of atherogenesis. *Atherosclerosis*. 1986;60:131–139.

34. Wen Y, Leake DS. Low density lipoprotein undergoes oxidation within lysosomes in cells. *Circ Res*. 2007;100:1337–1343.

35. Ishibashi M, Filomenko R, Rébé C, Chevriaux A, Varin A, Derangère V, Bessède G, Gambert P, Lagrost L, Masson D. Knock-down of the oxysterol receptor LXRα impairs cholesterol efflux in human primary macrophages: Lack of compensation by LXRβ activation. *Biochem Pharmacol*. 2013;33:1171–1179.

36. Boyle JJ, Johns M, Kampfer T, Nguyen AT, Game L, Schaer DJ, Mason JC, Haskard DO. Activating transcription factor 1 directs Mhem atheroprotective macrophages through coordinated iron handling and foam cell protection. *Circ Res*. 2012;110:20–33.

NOVELTY AND SIGNIFICANCE

What is known?

- Monocytes differentiate in functionally distinct pro-inflammatory "classical" M1 macrophages and anti-inflammatory "alternative" M2 macrophages.

- CD68+MR+ M2 macrophages are present in human atherosclerotic lesions.

- Macrophages in human atherosclerotic lesions accumulate iron.

What new information does this article contribute?

- Iron preferentially accumulates in M2 macrophages in human atherosclerotic plaques.

- Upon iron exposure, M2 macrophages acquire a phenotype favouring iron release, via a strong increase in ferroportin expression.

- In human atherosclerotic plaques, CD68+MR+ macrophages accumulate oxidized lipids, which activate Liver X Receptors (LXRα and LXRβ) and induce the expression of their target genes.

- LXR activation induces nuclear factor erythroid 2-like 2 (NRF2) and increases ferroportin expression, which, together with a decrease in hepcidin mRNA levels, promotes iron export.

Monocytes infiltrate the intima of large arteries and differentiate into macrophages. Macrophages are functionally heterogeneous cells adapting their phenotype to the cytokine environment. Th1 cytokines promote the M1 phenotype, while Th2 cytokines trigger an "alternative" M2 phenotype. In atherosclerotic plaques, macrophages are the major cells accumulating iron, which can exert pro-oxidant activities. In this study we have characterized the distribution and metabolism of iron in macrophage sub-populations in human atherosclerotic plaques and determined whether iron homeostasis is under the control of the nuclear receptors LXR.
We found that iron is mostly present in CD68+MR+ alternative M2 macrophage-enriched areas. *In vitro* IL-4 polarized M2 macrophages display a gene expression profile favouring iron accumulation. Upon iron exposure, M2 macrophages acquire the ability to release iron, via the induction of ferroportin expression. In human atherosclerotic plaques, CD68+MR+ macrophages accumulate oxidized lipids, which activate LXR. Moreover, in iron-loaded M2 macrophages, LXR activation increases ferroportin expression by a nuclear factor erythroid 2-like 2 (NRF2)-dependent mechanism, which, together with a decrease of hepcidin mRNA, promotes iron export. Our work identifies a role for M2 macrophages in iron handling, a process regulated by LXR activation.

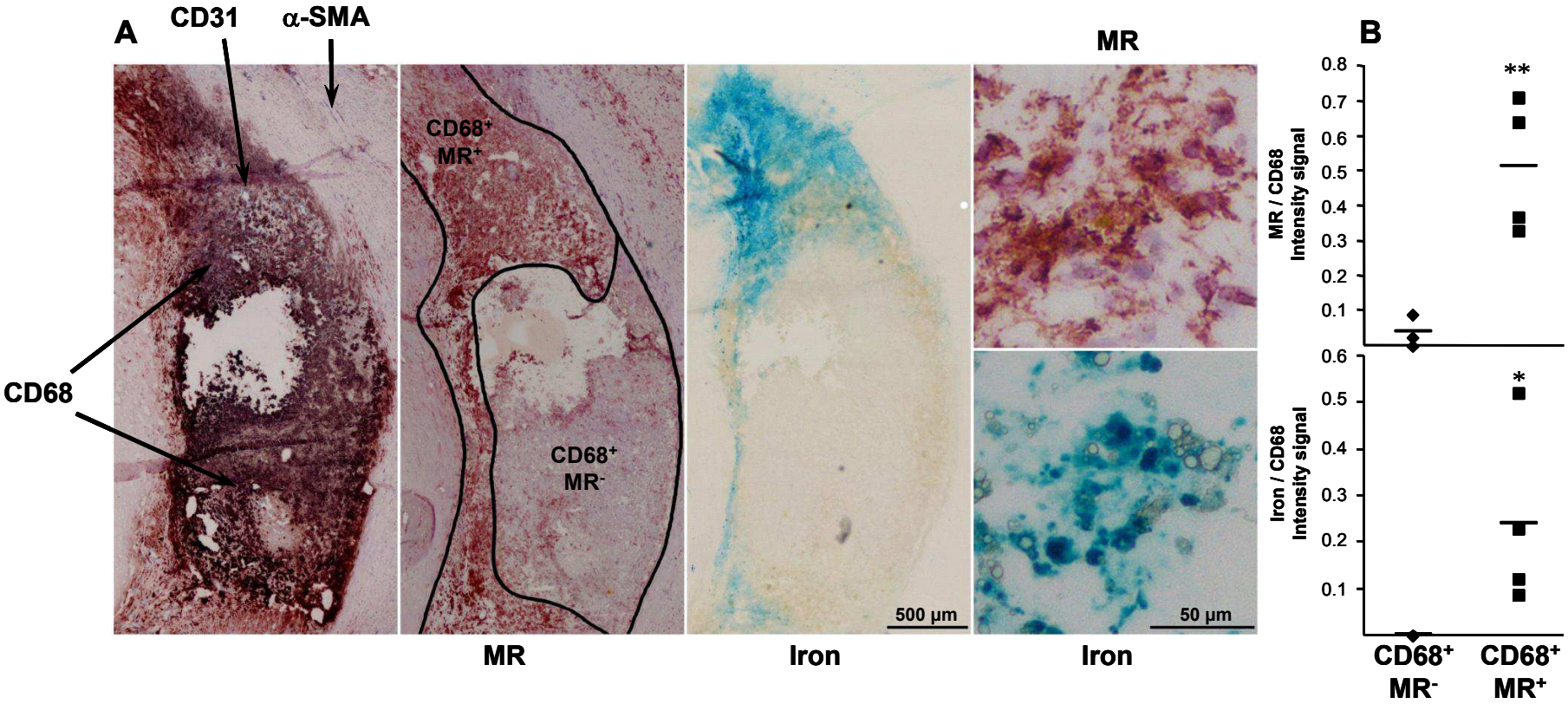

Figure 1. CD68+MR+ macrophages colocalize with iron depots in human atherosclerotic plaques
(A) Left panel: Representative immunostaining for CD68 (red), PECAM-1/CD31 (blue), a-smooth muscle actin (a-SMA, grey) in human carotid atherosclerotic lesions. Right panels: higher magnifications for MR staining (red) and iron depots (blue). Scale bars are shown.
(B) Quantification of the intensities of MR (top) and iron (bottom) staining in CD68+MR+ and CD68+MR- macrophage-enriched areas of human atherosclerotic plaques. Each point corresponds to a single atherosclerotic plaque. The mean value (horizontal bar) and statistical significance of differences are indicated (*t* test; **P*<0.05, ***P*<0.01).

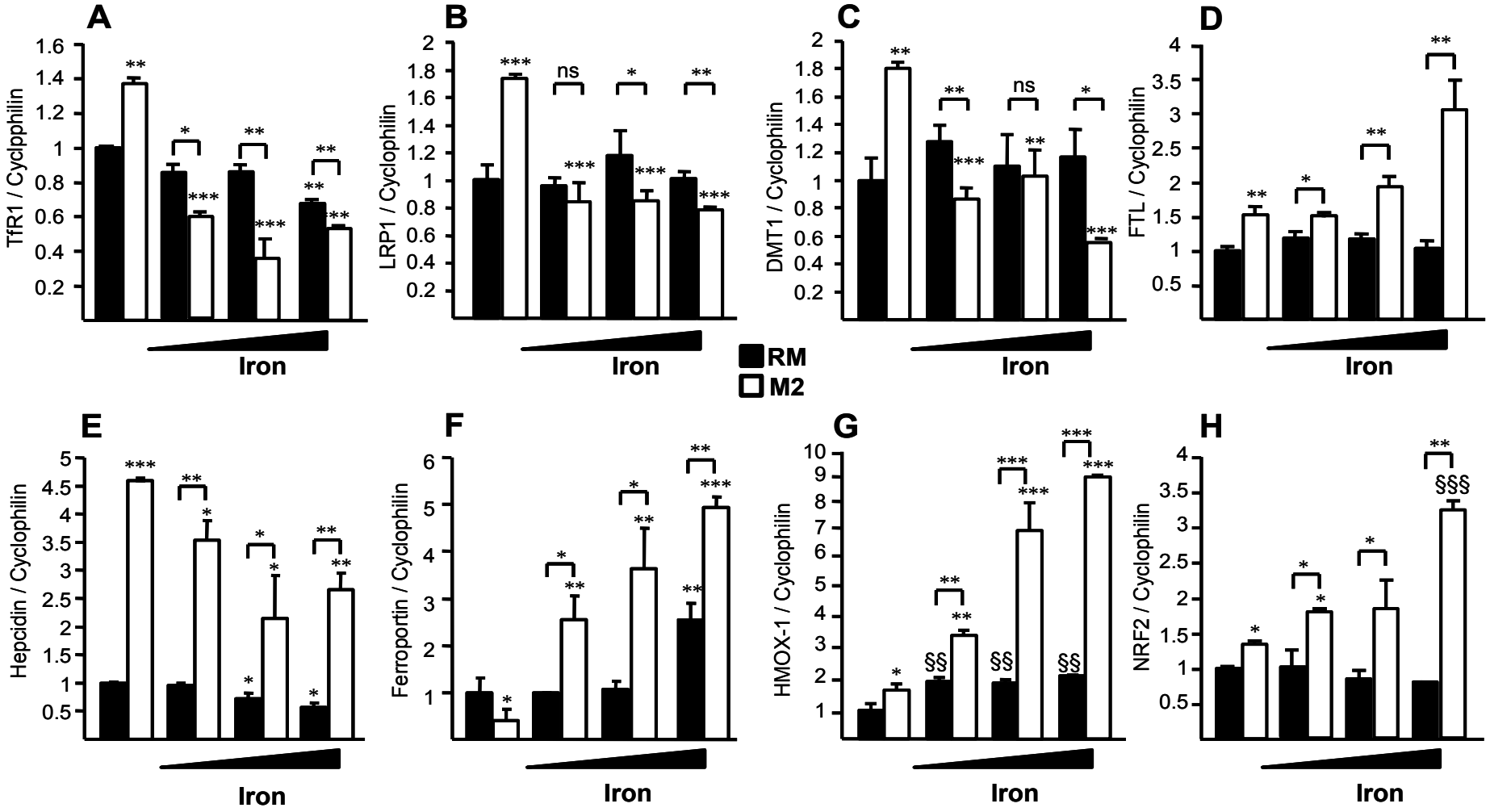

Figure 2. Iron loading regulates the expression of genes related to iron metabolism mainly in M2 macrophages
RM and M2 macrophages were loaded or not with increasing iron concentrations ($FeCl_3$ 25, 50, 100 µmol/L). TfR1 (A), LRP1 (B), DMT1 (C), FTL (D), hepcidin (E), ferroportin (F) HMOX-1 (G) and NRF2 (H) mRNA levels were measured by Q-PCR and normalized to cyclophilin mRNA and results expressed as mean ± SD of triplicate determination relative to the levels in RM without iron set at 1. Statistical significant differences are indicated (*t* test; RM treated iron vs RM control: §*P*<0.05, §§*P*<0.01, §§§*P*<0.001, M2 treated iron vs M2 control: **P*<0.05, ***P*<0.01, ****P*<0.001).

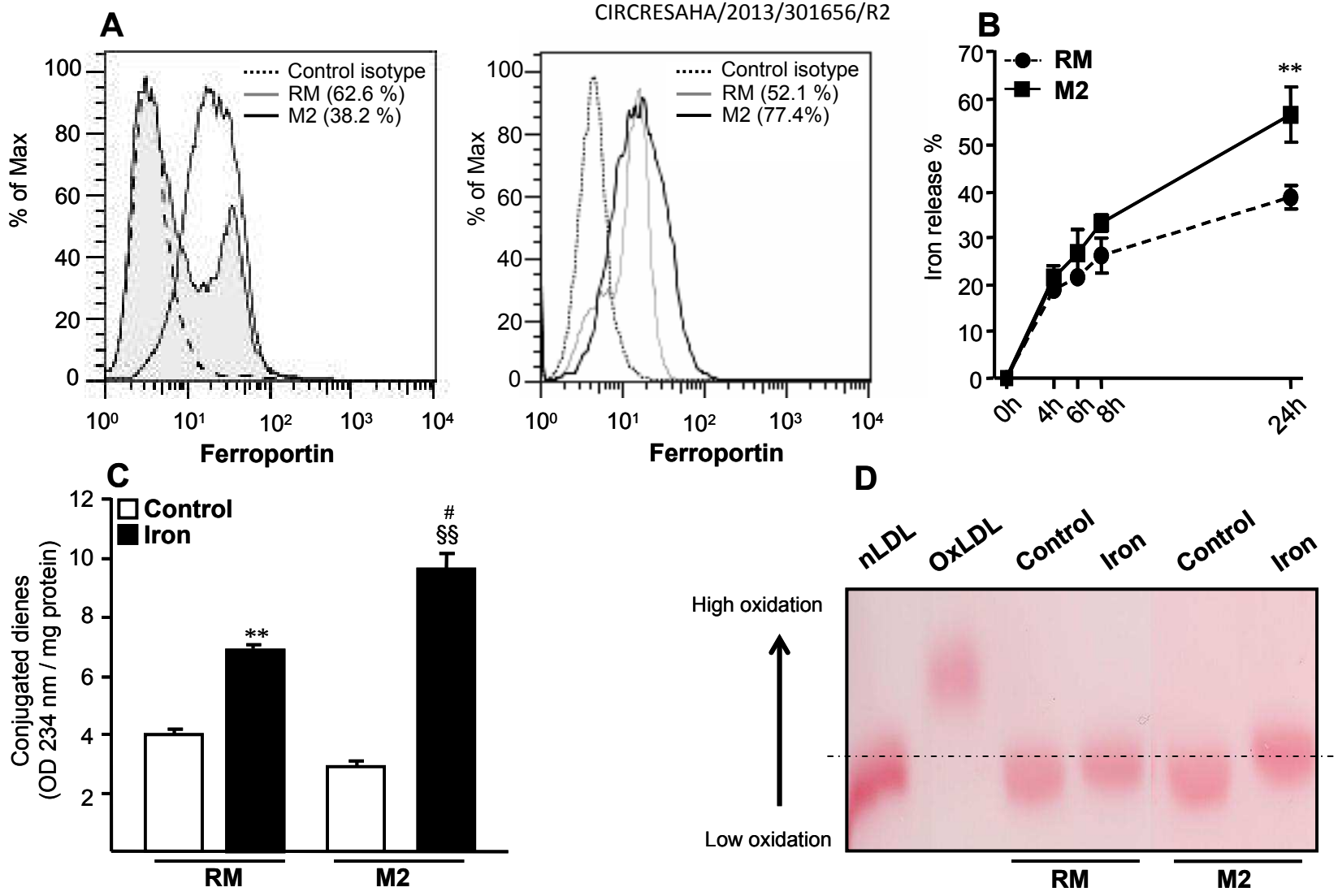

Figure 3. Iron-loaded M2 macrophages display higher iron export capacity and enhanced LDL oxidation

(A) Analysis of ferroportin protein expression in unloaded (left panel) and iron-loaded (right panel) RM and M2 macrophages. (B) RM and M2 macrophages were iron-loaded ($FeCl_3$ 100µmol/L, 24h) followed by wash-out periods (4, 6, 8 and 24h; ANOVA and *t* test; ***P*<0.01). Intracellular and medium iron content was measured by ferrozine assay and iron export calculated as described in Materials and Methods. (C) Macrophages loaded or not with iron were incubated with nLDL (1mg/ml). After a 24h wash-out period, LDL was isolated from medium and the conjugated dienes content (D) and electrophoretic mobility (E) measured. Cupper-oxidized LDL was used as positive control. Statistical significant differences are indicated (t test; RM iron *vs* RM control ***P*<0.01; M2 iron *vs* M2 control §§*P*<0.01; RM iron *vs* M2 iron #*P*<0.05).

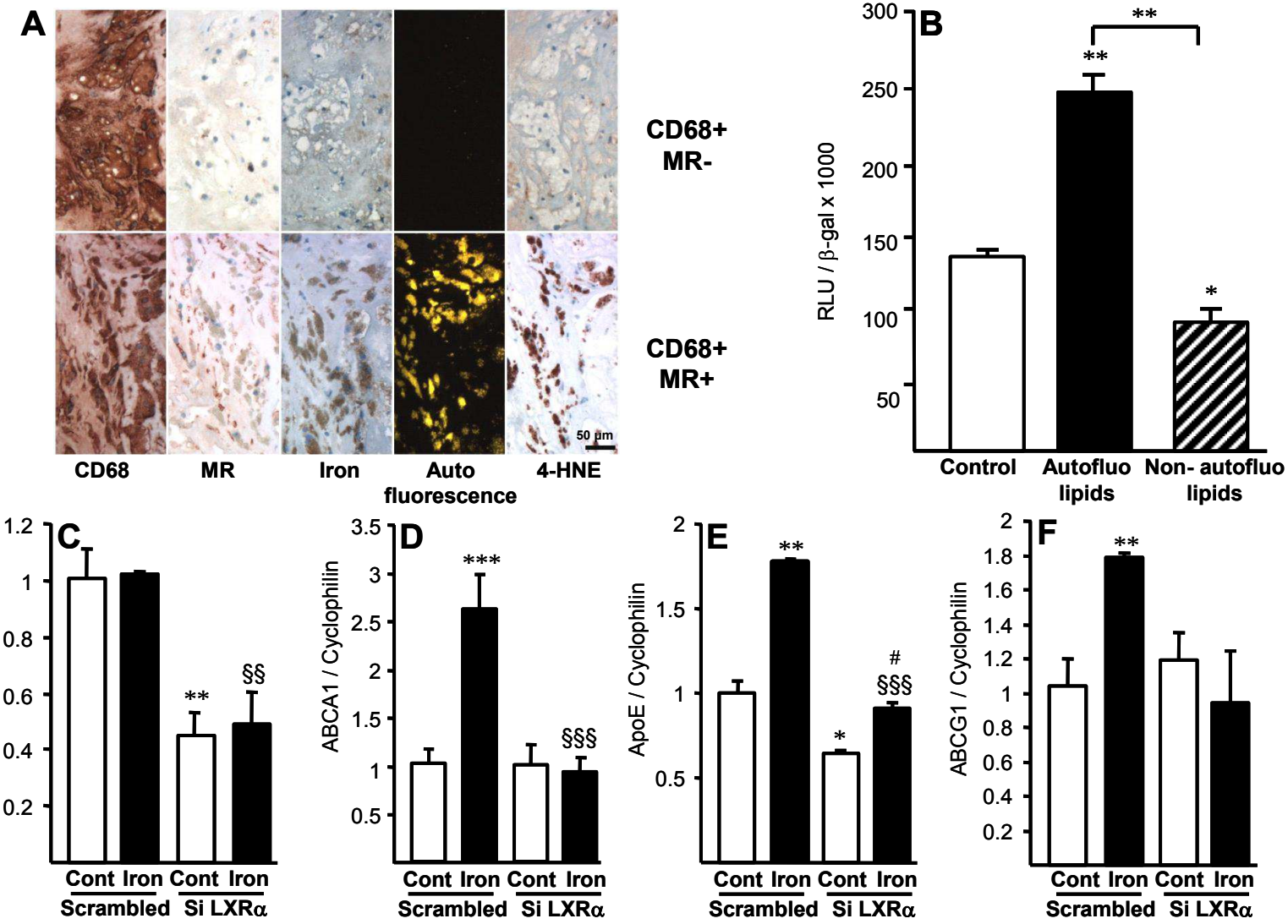

Figure 4. Oxidized lipids from human atherosclerotic plaques and iron loading induce LXRα transcriptional activity

(A) Representative immunostaining for CD68, MR and iron depots in human carotid atherosclerotic lesions. Oxidized lipids were revealed by autofluorescence or by 4-HNE immunostaining. (B) COS cells were transfected with LXRE-reporter and LXRα expression plasmids and treated with autofluorescent oxidized or non-autofluorescent lipids extracted from CD68+MR+ and from CD68+MR- macrophage-enriched areas of human atherosclerotic plaques, respectively. M2 macrophages were transfected with scrambled or LXRα siRNA, in the presence or in the absence of iron ($FeCl_3$ 100 µmol/L, 24h) and Q-PCR analysis of LXRα (C), ABCA1 (D), ApoE (E) and ABCG1 (F) performed. mRNA levels were normalized to cyclophilin mRNA and results expressed as mean ± SD of triplicate determination relative to the levels in scrambled siRNA transfected cells set at 1. Statistical significant differences are indicated (*t* test; scramble *vs* scramble iron or siLXRα control **P*<0.05, ***P*<0.01, ****P*<0.001; scramble iron *vs* siLXRα iron §§*P*<0.01, §§§*P*<0.001; control siLXRα vs LXRα iron # *P*<0.05).

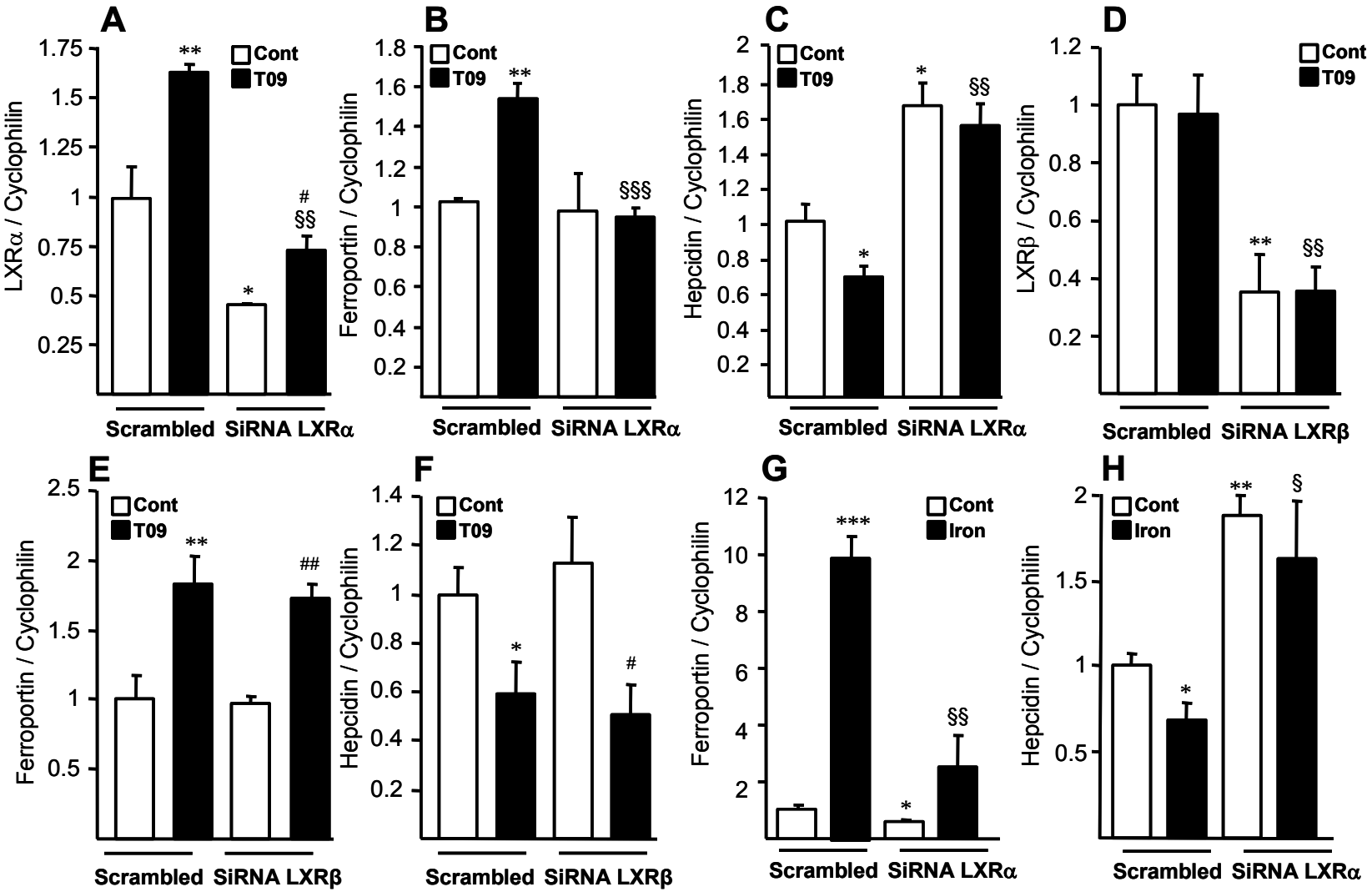

Figure 5. LXRα, but not LXRβ, controls the expression of genes involved in iron export

M2 macrophages were transfected with scrambled, LXRα or LXRβ siRNA, in the presence or in the absence of T09 (1 µmol/L) (A-F) or transfected with LXRα siRNA, in the presence or in the absence of iron ($FeCl_3$ 100 µmol/L, 24h) (G-H). Q-PCR analysis of LXRα (A), LXRβ (D), ferroportin (B,E,G) and hepcidin (C,F,H) mRNA levels were normalized to cyclophilin mRNA and results expressed as mean ± SD of triplicate determination relative to the levels in scrambled siRNA transfected cells set at 1. Statistical significant differences are indicated (*t* test; scramble *vs* scramble T09 or siLXR control **P*<0.05, ***P*<0.01, ****P*<0.001; scramble T09/iron *vs* siLXR T09/iorn §*P*<0.05, §§*P*<0.01, §§§*P*<0.001, siLXR *vs* siLXR T09; #*P*<0.05, ##*P*<0.01).

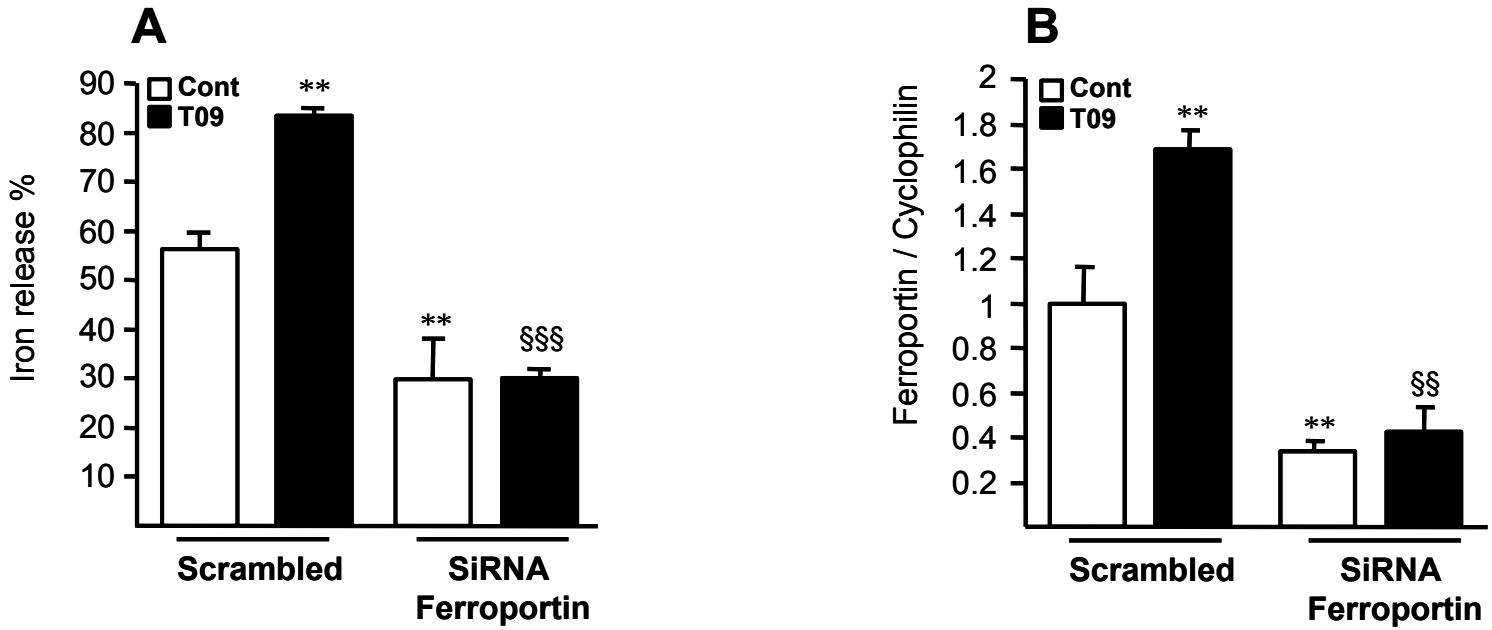

Figure 6. LXRα activation enhances iron export via ferroportin

(A) M2 macrophages were transfected with scrambled or ferroportin siRNA and loaded with iron ($FeCl_3$ 100µmol/L, 24h). After medium removal, cells were treated with or without T09 (1µmol/L, 24h). Iron release was calculated as described. (B) Iron-loaded M2 macrophages were transfected with scrambled or ferroportin siRNA in the absence or in the presence of T09 (24h, 1 µmol/L). Ferroportin mRNA levels were measured by Q-PCR and normalized to cyclophilin mRNA and results expressed as mean ± SD of triplicate determination relative to the levels in scrambled siRNA transfected cells set at 1. Statistical significant differences are indicated (*t* test; scramble control *vs* scramble T09 or siRNA ferroportin control ***P*<0.01; scramble T09 *vs* siRNA ferroportin T09 §§*P*<0.01, §§§*P*<0.001).

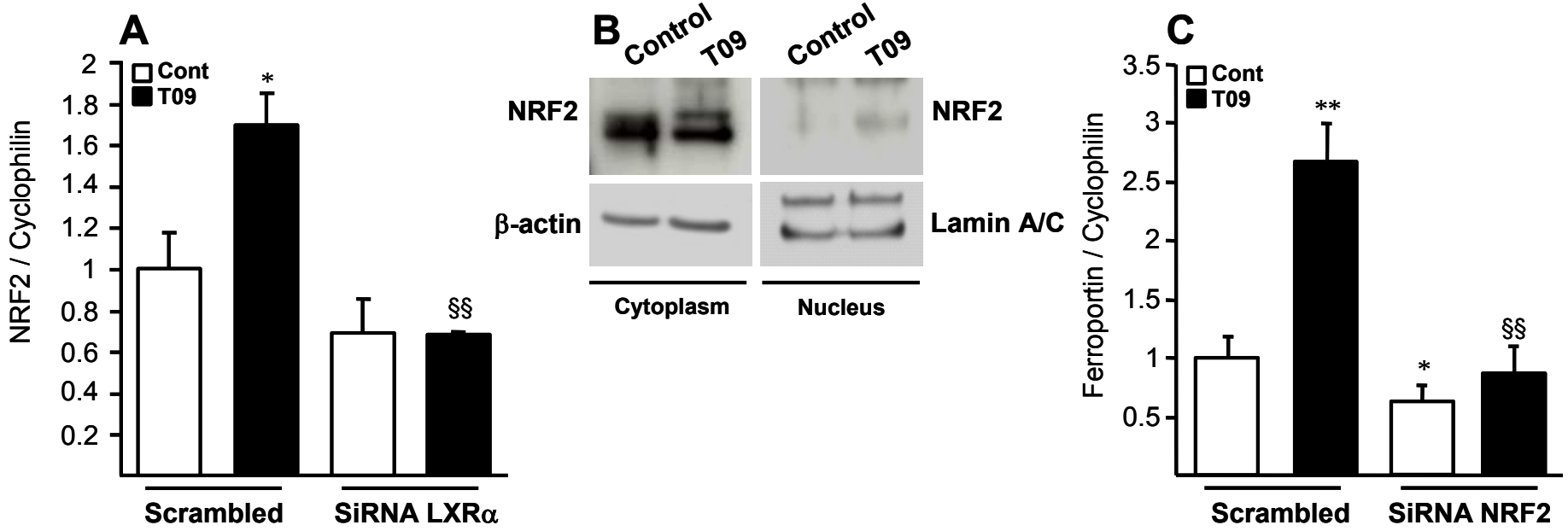

Figure 7. LXRα activation induces ferroportin expression via NRF2

M2 macrophages were transfected with scrambled, LXRα or NRF2 siRNA, treated or not with T09 (1 µmol/L). mRNA levels of NRF2 (A) and ferroportin (C) were normalized to cyclophilin mRNA and results expressed as mean ± SD of triplicate determination relative to the levels in scrambled siRNA transfected cells set at 1. (B) M2 macrophages were treated or not with T09 (1µmol/L, 24h) and NRF2 protein was measured in the cytoplasmic and nuclear fraction. Statistical significant differences are indicated (*t* test; scramble control *vs* scramble T09 or siRNA control **P*<0.05, ***P*<0.01; scramble T09 *vs* siRNA T09 §§*P*<0.01).

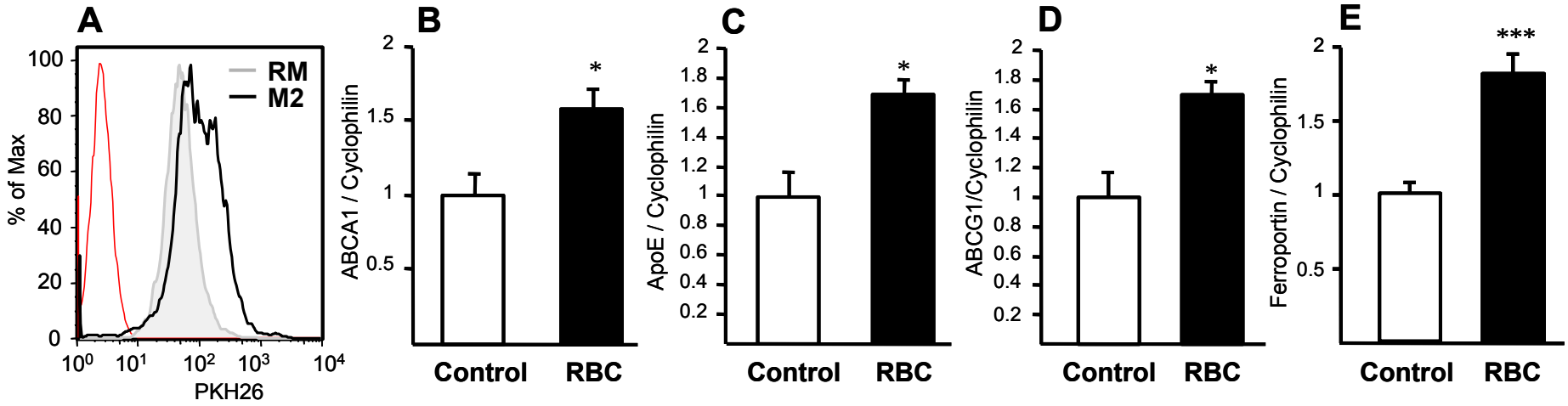

Figure 8. M2 macrophages efficiently phagocytose senescent erythrocytes
(A) Phagocytosis of senescent PKH26-labelled erythrocytes (RBC) in RM and M2 macrophages after 16h of incubation. Red histogram: isotype control. Q-PCR analysis of ABCA1 (B), ABCG1 (C), ApoE (D), and ferroportin (E) in M2 macrophages in the absence or in the presence of senescent RBC. mRNA levels were normalized to cyclophilin mRNA and results expressed as mean ± SD of triplicate determination relative to the levels in RM set at 1. Statistical significant differences are indicated (*t* test; **P*<0.05, ****P*<0.001).